

1    **Classification**

2    Major Category: Biological Sciences

3    Minor Category: Microbiology

4

5    **The Evolution of Fluoroquinolone-Resistance in *Mycobacterium tuberculosis* is**  
6    **Modulated by the Genetic Background**

7

8    Rhastin A. D. Castro<sup>1,2</sup>, Amanda Ross<sup>1,2</sup>, Lujeko Kamwela<sup>1,2</sup>, Miriam Reinhard<sup>1,2</sup>, Chloé  
9    Loiseau<sup>1,2</sup>, Julia Feldmann<sup>1,2</sup>, Sonia Borrell<sup>1,2</sup>, Andrej Trauner<sup>1,2,†</sup>, and Sébastien Gagneux<sup>1,2,\*</sup>

10

11    <sup>1</sup>Swiss Tropical and Public Health Institute, Basel, Switzerland

12    <sup>2</sup>University of Basel, Basel, Switzerland

13

14    <sup>\*,†</sup>Corresponding authors

15    Socinstrasse 57, 4051 Basel, Switzerland

16    T: +41 61 284 6983

17    F: +41 61 284 8101

18    Email: [sebastien.gagneux@swisstph.ch](mailto:sebastien.gagneux@swisstph.ch)

19    Email: [andrey.trauner@swisstph.ch](mailto:andrey.trauner@swisstph.ch)

20

21    **Abstract**

22       Fluoroquinolones (FQ) form the backbone in experimental treatment regimens against  
23       drug-susceptible tuberculosis. However, little is known on whether the genetic variation present

24 in natural populations of *Mycobacterium tuberculosis* (*Mtb*) affects the evolution of FQ-  
25 resistance (FQ-R). To investigate this question, we used a set of *Mtb* strains that included nine  
26 genetically distinct drug-susceptible clinical isolates, and measured their frequency of resistance  
27 to the FQ ofloxacin (OFX) *in vitro*. We found that the *Mtb* genetic background led to differences  
28 in the frequency of OFX-resistance (OFX-R) that spanned two orders of magnitude and  
29 substantially modulated the observed mutational profiles for OFX-R. Further *in vitro* assays  
30 showed that the genetic background also influenced the minimum inhibitory concentration and  
31 the fitness effect conferred by a given OFX-R mutation. To test the clinical relevance of our *in*  
32 *vitro* work, we surveyed the mutational profile for FQ-R in publicly available genomic sequences  
33 from clinical *Mtb* isolates, and found substantial *Mtb* lineage-dependent variability. Comparison  
34 of the clinical and the *in vitro* mutational profiles for FQ-R showed that 45% and 19% of the  
35 variability in the clinical frequency of FQ-R *gyrA* mutations in Lineage 2 and Lineage 4 strains,  
36 respectively, can be attributed to how *Mtb* evolves FQ-R *in vitro*. As the *Mtb* genetic background  
37 strongly influenced the evolution of FQ-R *in vitro*, we conclude that the genetic background of  
38 *Mtb* also impacts the evolution of FQ-R in the clinic.

39

40 Keywords: *Mycobacterium tuberculosis*, antimicrobial resistance, evolution, fluoroquinolones,  
41 epistasis

42

### 43 **Significance**

44 Newer generations of fluoroquinolones form the backbone in many experimental  
45 treatment regimens against *M. tuberculosis* (*Mtb*). While the genetic variation in natural  
46 populations of *Mtb* can influence resistance evolution to multiple different antibiotics, it is

47 unclear whether it modulates fluoroquinolone-resistance evolution as well. Using a combination  
48 of *in vitro* assays coupled with genomic analysis of clinical isolates, we provide the first evidence  
49 illustrating the *Mtb* genetic background's substantial role in fluoroquinolone-resistance evolution,  
50 and highlight the importance of bacterial genetics when studying the prevalence of  
51 fluoroquinolone-resistance in *Mtb*. Our work may provide insights into how to maximize the  
52 timespan in which fluoroquinolones remain effective in clinical settings, whether as part of  
53 current standardized regimens, or in new regimens against *Mtb*.

54

## 55 **Introduction**

56 Antimicrobial resistance (AMR) poses a major threat to our ability to treat infectious  
57 diseases (1, 2). The rise of AMR is a complex phenomenon with a broad range of contributing  
58 socioeconomic and behavioural factors (3–7). However, the emergence of AMR within any  
59 pathogen population is ultimately an evolutionary process (8, 9). This evolutionary process is  
60 influenced by multiple factors, including drug pressure and pathogen genetics. Firstly, the drug  
61 type and drug concentration can affect the type and relative frequencies of AMR mutations  
62 observed in a given pathogen population (also known as the mutational profile for AMR) (9–14).  
63 Secondly, pathogen populations comprise genetically distinct strains, and this genetic variation  
64 may also influence AMR evolution (15–17). Different pathogen genetic backgrounds can have  
65 different baseline susceptibilities to a given drug (18, 19), which consequently can affect patient  
66 treatment outcomes (20). The genetic background has also been shown to modulate the  
67 acquisition and prevalence of AMR (11, 15, 21, 22), the mutational profile for AMR (11, 15, 16,  
68 23), and the phenotypic effects of AMR mutations (24–28). Studying the interplay between

69 pathogen genetics and drug pressure is therefore important in understanding how to restrict the  
70 prevalence of AMR in pathogen populations.

71 AMR in *Mycobacterium tuberculosis* (*Mtb*), the aetiological agent of human tuberculosis  
72 (TB), is of particular importance. *Mtb* infections globally cause the highest rate of mortality due  
73 to a single infectious agent both in general, and due to AMR specifically (29). Although the  
74 genetic variation in *Mtb* is small compared to other bacterial pathogens (17, 30), several studies  
75 have shown that this limited genetic variation influences AMR phenotypes and prevalence (15,  
76 17, 24, 28, 31). The global genetic diversity of *Mtb* comprises seven phylogenetic lineages (17,  
77 30), and *Mtb* strains belonging to the Lineage 2 Beijing/W genetic background have repeatedly  
78 been associated with multidrug-resistant TB (MDR-TB; defined as an infection from an *Mtb*  
79 strain that is resistant to at least isoniazid and rifampicin) both *in vitro* and in clinical settings (4,  
80 11, 15, 21, 22).

81 One strategy to reduce the emergence of AMR in *Mtb* is the development of new, shorter  
82 treatment regimens (32, 33). Many such experimental regimens use third- or fourth-generation  
83 fluoroquinolones (FQ) against drug-susceptible *Mtb* (32–36). However, FQs have long been  
84 integral to treating MDR-TB (37), and the previous use of FQ has led to the emergence of FQ-  
85 resistance (FQ-R) in clinical strains of *Mtb* (7, 38–40). FQ-R is one of the defining properties of  
86 extensively drug-resistant TB (XDR-TB), and XDR-TB accounts for 8.5% of MDR-TB cases  
87 (29). Understanding how FQ-R is acquired in natural populations of *Mtb* may allow for the  
88 development of tools or strategies to mitigate further increases in FQ-R prevalence.

89 In *Mtb*, the sole target of FQ is DNA gyrase (10, 38, 41–43). Consequently, clinically  
90 relevant FQ-R in *Mtb* is primarily due to a limited set of chromosomal mutations located within  
91 the “quinolone-resistance-determining region” (QRDR) of the *gyrA* and *gyrB* genes, which

92 encode DNA gyrase (22, 38, 39). No horizontal gene-transfer (HGT) or plasmid-based resistance  
93 to FQ has been documented in *Mtb* (44, 45). Studying FQ-R evolution in *Mtb* populations thus  
94 provides a promising setting for elucidating how the genetic background may affect the  
95 emergence and maintenance of clinically relevant chromosomal AMR mutations in bacterial  
96 populations.

97 While a great deal of literature exists on the biochemical mechanisms leading to the FQ-R  
98 phenotype in *Mtb* (10, 41–43, 46, 47), little is known on the evolutionary dynamics of FQ-R in  
99 different populations of *Mtb*. Given that antimicrobial regimens against *Mtb* infections use  
100 standardized, empirical dosing strategies (29), it is unclear whether different *Mtb* genetic  
101 backgrounds would acquire FQ-R at the same frequency when exposed to the same antimicrobial  
102 concentration. Whether the *Mtb* genetic background would also modulate the mutational profile  
103 for FQ-R, or the phenotypic effects of FQ-R mutations, is unknown. Such knowledge may  
104 provide insights on how to maintain or prolong the efficiency of FQs against different genetic  
105 variants of *Mtb* in the clinic.

106 In this study, we tested whether the *Mtb* genetic background plays a role in the evolution  
107 of FQ-R. Specifically, we showed that the *Mtb* genetic background can lead to differences in the  
108 frequency of FQ-R emergence that span two-orders of magnitude, as well as substantially  
109 modulate the mutational profile for FQ-R. We further demonstrated that the phenotypic effects of  
110 clinically relevant FQ-R mutations differed depending on the *Mtb* genetic background they were  
111 present in. Analysis of publicly available genomic sequences from clinical *Mtb* isolates also  
112 revealed a positive association between the FQ-R mutational profiles observed *in vitro* and the  
113 mutational profiles observed in the clinic. Taken together, we showed that the *Mtb* genetic  
114 background had a considerable role in evolution of FQ-R in the clinic.

115

116 **Results**

117 **Frequency of ofloxacin-resistance in *M. tuberculosis* is strain-dependent**

118 We first tested for whether the *Mtb* genetic background led to differences in the frequency  
119 of FQ-R acquisition. To do so, we performed a Luria-Delbrück fluctuation analysis on nine drug-  
120 susceptible and genetically distinct *Mtb* clinical strains belonging to Lineage 1 (L1), Lineage 2  
121 (L2) and Lineage 4 (L4) (See SI Appendix, Table S1) (17, 30, 48, 49). We measured their  
122 frequency of resistance *in vitro* to the FQ ofloxacin (OFX), as OFX was used extensively to treat  
123 MDR-TB patients in the past. Given that anti-TB treatment regimens use standardized drug  
124 concentrations (29), we also measured the frequency of resistance to the same concentration of  
125 OFX (4  $\mu$ g/mL) for all nine strains. We observed significant strain-dependent variation in the  
126 frequency of OFX-resistance (OFX-R) at 4  $\mu$ g/mL, with the difference spanning two orders of  
127 magnitude (Fig. 1A;  $P = 2.2 \times 10^{-16}$ , Kruskal-Wallis). Several of the nine drug-susceptible *Mtb*  
128 strains contained missense substitutions in DNA gyrase that are not associated with FQ-R (See SI  
129 Appendix, Table S2) (49). These mutations are phylogenetic markers that reflect the population  
130 structure of *Mtb* and cannot be avoided if strains from different *Mtb* lineages are used (17, 30).  
131 We found no evidence for any associations between the presence a given phylogenetic DNA  
132 gyrase missense mutation and the frequency of OFX-R acquired.

133 The concentration of the antimicrobial can affect the observed frequencies of AMR in *Mtb*  
134 (10, 11, 13). Therefore, we tested whether changing the selective concentration of OFX would  
135 affect the relative differences in strain-specific OFX-R frequencies. For the sake of simplicity, we  
136 tested only two strains, with each strain at the opposite extremes of the frequency of resistance to  
137 4  $\mu$ g/mL OFX, as shown in Fig. 1A: N0157 (high OFX-R frequency) and N0145 (low OFX-R

138 frequency). We found that the frequency of OFX-R remained one to two-orders of magnitude  
139 higher in N0157 than in N0145 across all the concentrations we tested (Fig. 1B,  $P = 2.46 \times 10^{-5}$   
140 for 2  $\mu\text{g/mL}$  OFX, and  $P = 4.03 \times 10^{-6}$  for 8  $\mu\text{g/mL}$  OFX, Wilcoxon rank-sum test). The N0157  
141 strain had nearly confluent growth at 2  $\mu\text{g/mL}$  OFX, which is the OFX concentration that has  
142 been shown to inhibit 95% of *Mtb* strains that have not been previously exposed to OFX, but  
143 does not inhibit *Mtb* strains that are considered resistant to OFX in the clinic (18, 19). This  
144 suggested that N0157 has low-level resistance to OFX, despite having no mutation in the QRDR.  
145 Meanwhile, at 8  $\mu\text{g/mL}$  OFX, we observed only four resistant colonies for N0145 across all  
146 samples, with all colonies arising within the same culture.

147 The variation in OFX-R frequencies when selecting on the same concentration of OFX  
148 may be driven by several, non-exclusive biological factors. Firstly, the *Mtb* strains we tested may  
149 have different baseline DNA mutation rates. Secondly, the number and relative frequency of  
150 potential mutations that confer OFX-R may vary depending on the *Mtb* genetic background.  
151 Thirdly, the relative cost of OFX-R mutations may differ between *Mtb* genetic backgrounds. As  
152 the observed frequency of OFX-R in *Mtb* is likely the result from a combination of multiple  
153 factors, we took advantage of the fact that we had identified strains with a range of OFX-R  
154 frequencies. We selected three representative strains with significantly different OFX-R  
155 frequencies: N0157, N1283, and N0145. These strains had a high, mid-, and low frequency of  
156 OFX-R, respectively (Fig. 1A). We then explored the relative contributions of each biological  
157 factor listed above in driving the variation in OFX-R across genetically distinct *Mtb* strains.

158  
159 **Mutation rate differences do not drive the *in vitro* variation in ofloxacin-resistance**  
160 **frequency in *M. tuberculosis***

161 We first tested for the presence of differential mutation rates between our panel of *Mtb*  
162 strains in Fig. 1A. Mutations in *dnaE*, which encodes the replicative DNA polymerase and serves  
163 as the major replicative exonuclease in *Mtb*, have been shown to confer a hypermutator  
164 phenotype in *Mtb* in the absence of environmental stress (50, 51). While *dnaE* mutations were  
165 present in the genomic data of our panel of drug-susceptible *Mtb* strains (See SI Appendix, Table  
166 S2) (49), none were in the polymerase and histidinol phosphatase domain of DnaE, the region  
167 where mutations would impart a hypermutator phenotype (50, 51). We did not test for the  
168 presence of *dnaE* mutations in the resistant colonies following the fluctuation analysis, as we  
169 reasoned that the likelihood of gaining both a *dnaE* and a *gyrA* double mutation within this  
170 relatively short period is extremely low as to be considered negligible. To test for mutation rate  
171 variation *in vitro*, we again conducted a fluctuation analysis on N0157, N1283, and N0145 (the  
172 high-, mid-, and low-frequency OFX-R strains, respectively), but used streptomycin (STR; 100  
173 µg/mL) instead of OFX. We hypothesized that if the frequency of OFX-R is driven by  
174 differential mutation rates, then we should expect similar differences in the frequency of STR-  
175 resistance (STR-R). However, we observed no evidence for differences in the frequency of STR-  
176 R between the strains tested (Fig. 2,  $P = 0.135$ , Kruskal-Wallis; See SI Appendix, Table S3). This  
177 suggested that the observed differences in frequency of resistance are specific to OFX, and that  
178 there are limited, if any, inherent differences in mutation rate between the *Mtb* strains tested.

179

180 **Mutational profile for ofloxacin-resistance is highly strain-dependent**

181 We next determined the mutational profile for OFX-R for each strain used in the  
182 fluctuation analysis at 4 µg/mL OFX (Fig. 1A). The QRDR mutations in 680 *gyrA* and 590 *gyrB*  
183 sequences were identified in the resistant colonies. We observed that *gyrA* mutations made up

184 99.7% of the QRDR mutations observed (645 *gyrA* mutations, 2 *gyrB* mutations), and no QRDR  
185 double-mutants were present (See SI Appendix, Tables S4-S5). The mutational profiles for OFX-  
186 R were also highly strain-specific (Fig. 3A,  $P = 5.00 \times 10^{-4}$ , Fisher's exact test). Specifically, the  
187 GyrA A90V mutation was most prevalent in the high-frequency OFX-R strains, while GyrA  
188 D94G was most prevalent in all other strains. There was also a slight trend showing that strains  
189 with a greater number of unique *gyrA* mutations present also had higher rates of OFX-R (Fig. 1A;  
190 Fig. 3B).

191 The strain-dependent variation the mutational profile for OFX-R may be due to *gyrA*  
192 mutations conferring different resistance levels depending on the *Mtb* strain they are present in.  
193 To test this hypothesis, we first isolated OFX-R mutants carrying one of four possible GyrA  
194 mutations (G88C, A90V, D94G, or D94N) in the three strains used in Fig. 2: N0157, N1283, and  
195 N0145. The OFX MIC was determined for each of the twelve OFX-R mutant strains, along with  
196 their respective wild-type ancestors. We found that each parental wild-type strain had different  
197 susceptibilities to OFX, with N0157, N1283, and N0145 having OFX MICs of 2  $\mu\text{g/mL}$ , 0.6  
198  $\mu\text{g/mL}$ , and 0.5  $\mu\text{g/mL}$ , respectively (Fig. 4A; See SI Appendix, Table S6). This was consistent  
199 with the fluctuation analysis results shown in Fig. 1B. Furthermore, we observed that the OFX  
200 MIC conferred by a given *gyrA* mutation varied depending on the strain it was present in (Fig.  
201 4B; See SI Appendix, Table S6). For example, mutants in the N0157 strain generally had higher  
202 OFX MICs than mutants in either the N0145 or N1283 strains. The only mutation that deviated  
203 from this trend was GyrA G88C, which conferred a higher OFX MIC when in the N0145 strain.  
204 Notably, the GyrA A90V mutation conferred a resistance level equal to or greater than 4  $\mu\text{g/mL}$   
205 OFX in the N0157 and N1283 strains, but not in N0145. This was consistent with the presence of  
206 GyrA A90V in the OFX-R mutational profile for N0157 and N1283, but not in N0145, in the

207 fluctuation analysis using 4  $\mu$ g/mL OFX (Fig. 1A; Fig. 3). In summary, the differences in OFX  
208 MIC reflected the strain-dependent mutational profiles for OFX-R in *Mtb*, as expected.

209  
210 **Fitness of ofloxacin-resistance mutations are associated with their relative frequency *in vitro***

211 While the OFX MICs may determine which mutations may be observed in a fluctuation  
212 analysis, it is not the sole parameter to influence the OFX-R mutational profile for a given strain.  
213 We found that while the same *gyrA* mutation can be observed in two different *Mtb* strains, their  
214 relative frequencies may vary (Fig. 3). This variation may be due to the fitness of a given *gyrA*  
215 mutant being different across genetic backgrounds. To test this hypothesis, we used cell growth  
216 assays in antibiotic-free conditions to measure the *in vitro* fitness of our panel of OFX-R mutants  
217 relative to their respective parental wild-type ancestors. We observed that the relative fitness of  
218 the OFX-R mutants was modulated by both the *gyrA* mutation and the *Mtb* strain they were  
219 present in (Fig. 5A; See SI Appendix, Fig. S2-S3, Table S7). Furthermore, there was a positive  
220 association between the fitness of a given *gyrA* mutation with its relative frequency in the  
221 fluctuation analysis for the N0157 and N1283 strains (Fig. 5B,  $P = 0.03$  for N0157,  $P = 0.05$  for  
222 N1283). There was no evidence of an association in the N0145 background due to the lack of  
223 GyrA G88C and A90V mutants in its fluctuation analysis.

224 The results from Fig. 4 and Fig. 5, as well as the apparent lack of mutation rate  
225 differences between our strains (Fig. 1C), suggested that differential mutational profiles was an  
226 important contributor in the variation in OFX-R frequency in *Mtb*. These mutational profile  
227 differences appear to be driven by the *Mtb* genetic background's effect on both the MIC and the  
228 relative fitness cost of OFX-R mutations. We next explored whether these *in vitro* results would  
229 be relevant in clinical settings.

230

231 **Mutational profile for fluoroquinolone-resistance *in vitro* reflects clinical observations**

232 To explore the clinical relevance of our *in vitro* work, we surveyed the FQ-R mutational  
233 profile from publicly available *Mtb* genomes obtained from clinical isolates. FQs are generally  
234 used for treatment against MDR-TB (29). While it is unclear whether resistance mutations for  
235 isoniazid (INH) and/or rifampicin (RIF) predispose a strain to become FQ-R, the prevalence of  
236 FQ-R is heavily biased towards MDR-TB strains due to treatment practices. We therefore based  
237 our analyses on a collated dataset of 3,452 publicly available MDR-TB genomes (See SI  
238 Appendix, Table S8), which we confirmed to be MDR-TB based on the presence of known INH-  
239 and RIF-resistance mutations. This dataset provided a reasonable sampling of the overall genetic  
240 diversity of *Mtb*, as six of the seven known phylogenetic *Mtb* lineages were represented  
241 (Lineages 1 – 6) (17, 30). We catalogued their FQ-R mutational profiles, and found 950 FQ-R  
242 mutations in 854 genomes (See SI Appendix, Tables S9-S10), showing that multiple FQ-R  
243 mutations may be present in the genome of a single *Mtb* clinical isolate. The frequency of FQ-R  
244 differed between lineages, with the highest frequencies present in L2 and L4 strains ( $P < 2.2 \times$   
245  $10^{-16}$ , Chi-square Goodness of Fit Test). Moreover, we noticed a lineage-dependent mutational  
246 profile for FQ-R (Fig. 6,  $P = 3.00 \times 10^{-5}$ , Fisher's exact test; See SI Appendix, Fig. S4, Tables  
247 S10-S11). For example, while the GyrA D94G mutation was most prevalent in strains belonging  
248 to L1, L2, and Lineage 3 (L3), the GyrA A90V mutation was most prevalent in L4 and Lineage 6  
249 (L6).

250 We observed that the mutational profile for FQ-R in the fluctuation analysis experiments  
251 mimicked published clinical data. Firstly, *gyrA* mutations made up the large majority of FQ-R  
252 mutations *in vitro* (Fig. 3; See SI Appendix, Tables S4-S5) and 944 out of the 950 QRDR

253 mutations in the clinic (99.6%; Fig. 6; See SI Appendix, Table S10). The relative frequencies of  
254 *gyrA* mutations for each genetic background *in vitro* were also similar to their relative  
255 frequencies in the clinic. We compared the frequency of *gyrA* mutations from the OFX-R  
256 mutational profile assay in Fig. 3 to our genomic data survey in Fig. 6, but limited it to L2 and L4  
257 strains (the two lineages with the highest clinical frequencies of FQ-R). We observed a positive  
258 association between the frequency of a given *gyrA* mutation in our fluctuation analysis compared  
259 to the frequency in the clinic, with the association being significant for L2 strains (Fig. 7,  $P =$   
260 0.027 for L2,  $P = 0.130$  for L4, Fisher's exact test). Based on the adjusted  $R^2$  values, 45% of the  
261 variability in the clinical frequency of *gyrA* mutations in L2 strains and 19% of the variability in  
262 L4 strains can be attributed to how FQ-R evolves in *Mtb* *in vitro*. As the *in vitro* evolution of FQ-  
263 R is itself modulated by the *Mtb* genetic background, this provided evidence for the *Mtb* genetic  
264 background's role in the evolution of FQ-R in the clinic.

265

## 266 **Discussion**

267 Overall, we illustrate the *Mtb* genetic background's considerable role in the evolution of  
268 resistance to FQs, a clinically important antimicrobial. We first explored whether the genetic  
269 variation among natural populations of *Mtb* can influence FQ-R evolution *in vitro*. Specifically,  
270 considering that *Mtb* treatment regimens are based on standardized antimicrobial concentrations  
271 (29), we tested whether different genetic variants of *Mtb* would acquire FQ-R at the same  
272 frequency when exposed to the same concentration of FQ. Fluctuation analysis on nine,  
273 genetically distinct, drug-susceptible *Mtb* strains showed that the genetic background can have a  
274 drastic effect on the rate of OFX-R acquisition when using the same concentration of OFX (Fig.  
275 1). However, the effect of the genetic background on AMR frequencies observed here in the

276 context of OFX-R differed from those reported in previous work focusing on other antibiotics.  
277 Specifically, experimental evidence from Ford *et al.* suggested that L2 Beijing strains have a  
278 higher basal DNA mutation rate compared to L4 (11), which consequently leads to a higher  
279 frequency of resistance against INH, RIF and ethambutol, even after correcting for differences in  
280 AMR mutational profiles. Based on these results, one would expect that L2 Beijing strains would  
281 also show higher frequencies of FQ-R. However, this was not the case in our fluctuation analysis  
282 for OFX-R, as one of our L2 Beijing strains (N0145) repeatedly acquired the lowest frequency of  
283 OFX-R (Fig. 1). Moreover, we saw minimal, if any, DNA base-pair mutation rate differences  
284 between three *Mtb* strains with different *in vitro* OFX-R frequencies (Fig. 2). Contradicting  
285 results on the *in vitro* frequency of AMR in *Mtb* have been reported before, with other fluctuation  
286 analyses showing no difference in the frequency of RIF-R emergence between L2 Beijing and  
287 non-L2 Beijing strains (52). Although diverging in their results, these previous studies, together  
288 with the study conducted here, highlight the importance of the genetic background when testing  
289 for the frequency of AMR in *Mtb*. Furthermore, these results show that differential DNA  
290 mutation rate is not the only parameter relevant in determining the frequency of FQ-R in *Mtb*.

291 If DNA mutation rates do not contribute to the variation in OFX-R frequency, we  
292 hypothesized that differences in the phenotypic effects of OFX-R mutations, and their consequent  
293 effect on the mutational profiles for OFX-R, may be important contributors. By sequencing the  
294 QRDR from resistant colonies in our OFX fluctuation analysis, we observed strain-specific  
295 patterns in the mutational profiles for OFX-R (Fig. 3). This suggested that the mutational profile  
296 for FQ-R is not only a function of the FQ type and concentration (10, 14, 47, 53), but that  
297 epistatic interactions between a given FQ-R mutation and the genetic background may also play a  
298 role. Similar epistatic interactions have been observed in *Escherichia coli* (26), *Pseudomonas*

299 spp. (16, 27), *M. smegmatis* (54), and *Mtb* (24, 28, 31), where a given RIF-R *rpoB* mutation  
300 conferred differential MIC and fitness costs depending on the genetic background it occurred in,  
301 or on the presence of other AMR mutations. In line with these previous studies, we found that the  
302 OFX MIC and the fitness effect conferred by a given *gyrA* mutation varied significantly  
303 depending on the *Mtb* genetic background they occur in (Fig. 4; Fig. 5A; See SI Appendix, Table  
304 S6). These results support the hypothesis that epistasis plays a role in determining the strain-  
305 dependent OFX-R frequencies and mutational profiles observed during our fluctuation analyses  
306 (Fig. 3; Fig. 5B).

307 These epistatic interactions may have clinical consequences. A recent study has shown  
308 that drug-susceptible *Mtb* strains with higher MICs to INH and RIF were associated with  
309 increased risk of relapse following first-line treatment (20). Specific FQ-R *gyrA* mutations have  
310 also been associated with poorer treatment outcomes in MDR-TB patients (40, 55). Considering  
311 our observation that the *Mtb* genetic background affected both the OFX MICs and OFX-R  
312 mutational profiles (Fig. 3; Fig. 4; See SI Appendix, Tables S4-S6), the genetic background may  
313 therefore contribute to differences in patient treatment outcomes when using FQs as first-line  
314 drugs.

315 Using publicly available genomic data from *Mtb* clinical isolates, we observed significant  
316 lineage-dependent variation in the frequency of and mutational profiles for FQ-R (Fig. 6). As  
317 expected, the vast majority of FQ-R mutations were observed in *gyrA* (10, 22, 38, 39, 41–43).  
318 FQ-R was also most frequent in L2 and L4. This was also as expected, as strains from the L2  
319 Beijing sublineage are known to associate with MDR-TB (4, 15, 21, 22), while L4 strains are the  
320 most prevalent globally, including in regions classified as high-burden for TB (17, 29, 56, 57).  
321 Consequently, strains from L2 and L4 would be more exposed to FQs, leading to the higher FQ-

322 R frequencies observed in these two lineages. Furthermore, we observed that almost half of the  
323 variability in the clinical frequency of *gyrA* mutations of L2 strains can be explained by how *Mtb*  
324 evolves *in vitro* (Fig. 7). However, the *in vitro* FQ-R evolution could only account for 19% of the  
325 variability for *gyrA* mutation frequencies in clinical L4 strains. This suggested that while the *Mtb*  
326 genetic background can influence the evolution of FQ-R in the clinic, other factors (which may  
327 be independent of the *Mtb* genetic background) likely played strong roles as well.  
328 Epidemiological factors including socioeconomic disruptions, health system inefficiencies, and  
329 human behaviour are well known risk factors for the emergence and transmission of AMR in *Mtb*  
330 (3–7). Meanwhile, biological factors not explored in this study, such as antibiotic type and  
331 concentration (10–13, 46, 47), pharmacodynamic and pharmacokinetic features (58, 59), and the  
332 selective pressure of the host immune system (60), may also influence the evolution of FQ-R.

333 Our study is limited by the fact that our survey of clinical FQ-R frequencies involved a  
334 genomic dataset that was sampled by convenience. This dataset was used due to its public  
335 availability, and may not be fully representative of FQ-R frequencies in *Mtb* populations. We  
336 noted that lineage-specific frequencies of FQ-R were likely biased due to the overrepresentation  
337 L2 and L4 strains. Thus, to acquire a better understanding on which FQ-R mutations appeared  
338 and at what frequency they occurred at in different *Mtb* lineages, either more genomes from  
339 clinical isolates from other *Mtb* lineages must be made available, or a population-based study  
340 must be undertaken, preferably in a high burden MDR-TB region.

341 Exposure to quinolones have been shown to lead to SOS response-mediated mutagenesis,  
342 which can increase the rate of AMR acquisition, including resistance to quinolones themselves  
343 (53, 61, 62). Therefore, the strain-dependent OFX-R acquisition rates (Fig. 1) may be due to  
344 strain-dependent differences in the magnitude of quinolone-induced mutagenesis. We did not

345 explicitly test for this possibility. However, phylogenetic SNPs present in SOS response-related  
346 genes may lead to strain-dependent differences in quinolone-induced mutagenesis, and we  
347 observed no such SNPs present across our panel of drug-susceptible *Mtb* strains (See SI  
348 Appendix, Table S2) (49). Thus, we observed no genetic evidence for strain-specific SOS  
349 response-mediated mutagenesis. Furthermore, in *E. coli*, quinolone-induced quinolone-resistant  
350 mutations may only be observed after 5 days of incubation with quinolones, which is equivalent  
351 to approximately 225 generations for wild-type *E. coli* (53, 61). Meanwhile, our wild-type *Mtb*  
352 strains were incubated for 40 generations at most in the presence of OFX (see Materials and  
353 Methods; See SI Appendix, Table S7), making the likelihood of observing OFX-induced OFX-R  
354 mutants in our *in vitro* system extremely low.

355 Another limitation of our study is that fluctuation analyses only model AMR emergence.  
356 Long-term population dynamics also play an important role in AMR evolution (8, 12, 14). For  
357 example, population bottleneck events modulate AMR evolution during serial transfer  
358 experiments (14, 27, 63, 64), and have also been hypothesized to strongly influence *Mtb*  
359 evolution in the clinic (65). Thus, modeling FQ-R evolution in *Mtb* in epidemiological settings  
360 would benefit from the use of some measure of long-term population dynamics and between-host  
361 transmission. Nevertheless, the fitness of AMR mutants is an important factor in determining its  
362 evolutionary fate (8, 9, 12, 14, 26, 54, 64) and its potential for between-host transmission (63, 66,  
363 67). Considering that the *Mtb* genetic background modulated the fitness effect of FQ-R mutations  
364 (Fig. 5; See SI Appendix, Table S7), the genetic background may modulate how likely FQ-R  
365 mutants transmit between patients.

366 In conclusion, we illustrate how the genetic variation present in natural populations of  
367 *Mtb* modulates FQ-R evolution. Considering the non-random geographic distribution of different

368 *Mtb* genetic variants (17, 30), our work suggests that there may be regional differences in the rate  
369 of FQ-R emergence and FQ-R prevalence when using FQs as a first-line drug. We therefore  
370 highlight the importance of bacterial genetics in determining how FQ-R evolves in *Mtb* and, in  
371 general, how AMR evolves in pathogens.

372

373

374 **Materials and Methods**

375 **Collection of drug-susceptible clinical isolates of *M. tuberculosis* strains for *in vitro* studies**

376 We used nine genetically-distinct *Mtb* strains, with three strains from each of the  
377 following *Mtb* lineages: Lineage 1 (L1; also known as the East-Africa and India Lineage),  
378 Lineage 2 (L2; the East Asian Lineage), and Lineage 4 (L4; the Euro-American Lineage) (17,  
379 68). All strains were previously isolated from patients, fully drug-susceptible, and previously  
380 characterized by Borrell *et al.* (49) (See SI Appendix, Table S1).

381 Prior to all experimentation, starter cultures for each *Mtb* strain were prepared by  
382 recovering a 20  $\mu$ L aliquot from frozen stocks into a 10 mL volume of Middlebrook 7H9 broth  
383 (BD), supplemented with an albumin (Fraction V, Roche), dextrose (Sigma-Aldrich), catalase  
384 (Sigma-Aldrich), and 0.05% Tween® 80 (AppliChem) (hereafter designated as 7H9 ADC).  
385 These starter cultures were incubated until their optical density at wavelength of 600 nm (OD<sub>600</sub>)  
386 was approximately 0.50, and were then used for *in vitro* assays.

387

388 **Fluctuation analyses**

389 Fluctuation analyses were performed as described by Luria & Delbrück (48). Briefly, an  
390 aliquot from the starter cultures for each strain was used to inoculate 350 mL of 7H9 ADC to  
391 have an initial bacterial density of 5,000 colony forming units (CFU) per mL. This was  
392 immediately divided into 33 parallel cultures, each with 10 mL of culture volume aliquoted into  
393 individual 50 mL Falcon™ Conical Centrifuge Tubes (Corning Inc.). The parallel cultures were  
394 incubated at 37°C on standing racks, with re-suspension by vortexing (Bio Vortex V1, Biosan)  
395 every 24 hours. Cultures were grown until an OD<sub>600</sub> of between 0.40 to 0.65. Once at this density,  
396 final cell counts ( $N_t$ ) from three randomly chosen parallel cultures were calculated by serial

397 dilution and plating on Middlebrook 7H11 (BD), supplemented with oleic acid (AppliChem),  
398 albumin, and catalase (hereafter referred to as 7H11 OADC). To calculate the number of resistant  
399 colonies ( $r$ ), the remaining 30 parallel cultures not used for  $N_t$  determination were pelleted at 800  
400 g for 10 min. at 4°C using the Allegra X-15R Benchtop Centrifuge (Beckmann Coulter). The  
401 supernatants were discarded, and the bacterial pellets re-suspended in 300  $\mu$ L of 7H9 ADC. The  
402 re-suspensions were spread on 7H11 OADC plates supplemented with the relevant drug  
403 concentration (2, 4, or 8  $\mu$ g/mL of ofloxacin, or 100  $\mu$ g/mL streptomycin; Sigma). Resistant  
404 colonies were observed and enumerated after 21 to 35 days of incubation, depending on the *Mtb*  
405 strain. The estimated number of mutations per culture ( $m$ ) was estimated from the distribution of  
406 frequency of drug-resistance per cell ( $r_{dist}$ ) using the Ma, Sarkar, Sandri-Maximum Likelihood  
407 Estimator method (MSS-MLE) (69). The frequency of drug-resistance acquired per cell ( $F$ ) per  
408 strain was then calculated by dividing the calculated  $m$  values by their respective  $N_t$  values. The  
409 95% confidence intervals for each  $F$  were calculated as previously described by Rosche & Foster  
410 (69). Hypotheses testing for significant differences between the  $r_{dist}$  between strains for the  
411 fluctuation analyses at 4  $\mu$ g/mL of OFX (Fig. 1A) and at 100  $\mu$ g/mL of STR (Fig. 1C) were  
412 performed using the Kruskal-Wallis test; significant differences in the  $r_{dist}$  between strains in the  
413 fluctuation analyses at 2 and 8  $\mu$ g/mL (Fig. 1B) were tested for using the Wilcoxon rank-sum  
414 test. Statistical analyses were performed using the R statistical software (70).  
415

#### 416 **Determining the mutational profile for ofloxacin-resistance *in vitro***

417 From the parallel cultures plated on 4  $\mu$ g/mL of OFX (Fig. 1A), up to 120 resistant  
418 colonies per strain (at least 1 colony per plated parallel culture if colonies were present, to a  
419 maximum of 6) were transferred into 100  $\mu$ L of sterile deionized H<sub>2</sub>O placed in Falcon® 96-well

420 Clear Microplate (Corning Inc.). The bacterial suspensions were then heat-inactivated at 95°C for  
421 1 h, and used as PCR templates to amplify the QRDR in *gyrA* and *gyrB* using primers designed  
422 by Feuerriegel *et al.* (71). PCR products were sent to Macrogen, Inc. or Microsynth AG for  
423 Sanger sequencing, and QRDR mutations were determined by aligning the PCR product  
424 sequences against the H37Rv reference sequence (72). Sequence alignments were performed  
425 using the Staden Package, while the amino acid substitutions identification were performed using  
426 the Molecular Evolutionary Genetics Analysis Version 6.0 package. Fisher's exact test was used  
427 to test for significant differences between the strains' mutational profiles for OFX-R. Data  
428 analyses were performed using the R statistical software (70).

429

### 430 **Isolation of spontaneous ofloxacin-resistant mutants**

431 Spontaneous OFX-resistant mutants were isolated from strains belonging one of three  
432 genetic backgrounds: N0157 (L1, Manila sublineage; high frequency of OFX-R), N1283 (L4,  
433 Ural sublineage; mid-frequency of OFX-R), and N0145 (L2, Beijing sublineage; low frequency  
434 of OFX-R). To begin, we transferred 50 µL of starter cultures for each strain into separate culture  
435 tubes containing 10 mL of fresh 7H9 ADC. Cultures were incubated at 37°C until OD<sub>600</sub> of  
436 approximately 0.80, and pelleted at 800 g for 5 min at 4°C. The supernatant was discarded, and  
437 the pellet re-suspended in 300 µL of 7H9 ADC. The re-suspension was plated on 7H11 OADC  
438 (BD) supplemented with 2 µg/mL of OFX, and incubated until resistant colonies appeared  
439 (approximately 14 to 21 days). Resistant colonies were picked and re-suspended in fresh 10 mL  
440 7H9 ADC, and incubated at 37°C. Once the culture reached early stationary phase, two aliquots  
441 were prepared. The first aliquot was heat-inactivated at 95°C for 1 h, and the *gyrA* mutation  
442 identified by PCR and Sanger sequencing, as described in the mutational profile for OFX-R

443 assay. If the first aliquot harboured one of four OFX-r *gyrA* mutations (GyrA<sup>D94G</sup>, GyrA<sup>D94N</sup>,  
444 GyrA<sup>A90V</sup>, or GyrA<sup>G88C</sup>), the second aliquot was stored in -80°C for future use.

445 Prior to further experimentation with the spontaneously OFX-R mutant strains, starter  
446 cultures were prepared in the same manner as for the drug-susceptible strains.

447

448 **Drug susceptibility assay**

449 We determined the OFX-susceptibility levels of our spontaneous OFX-resistant mutants  
450 and their respective drug-susceptible ancestors by performing the colorimetric, microtiter plate-  
451 based Alamar Blue assay (73). Briefly, we used a Falcon® 96-well Clear Microplate, featuring a  
452 serial two-fold dilution of OFX. For drug-susceptible strains, a range of OFX concentration from  
453 15 µg/mL to 0.058 µg/mL was used. Meanwhile, for OFX-resistant strains, a range of 60 µg/mL  
454 to 0.234 µg/mL was used. Each well was inoculated with a 10 µL volume of starter culture to  
455 have a final inoculum of approximately  $5 \times 10^6$  CFU/mL. The plates were incubated at 37°C for  
456 10 days. Following incubation, 10 µL of Resazurin (Sigma) was added to each well, and the  
457 plates were incubated for another 24 h at 37°C. After this incubation period, plates were  
458 inactivated by adding 100 µL of 4% formaldehyde to every well. Measurement of fluorescence  
459 produced by viable cells was performed on SpectraMAX GeminiXPS Microplate Reader  
460 (Molecular Devices). The excitation wavelength was set at 536 nm, and the emission wavelength  
461 at 588 nm was measured. Minimum inhibitory concentration (MIC) for OFX was determined by  
462 first fitting a Hill curve to the distribution of fluorescence, and then defining the MIC as the  
463 lowest OFX concentration where the fitted Hill curve showed a  $\geq 95\%$  reduction in fluorescence.  
464 Two sets of experiments were performed for every strain, with three technical replicates per

465 experiment. Analyses of MIC data were performed and figures created using the numpy, scipy,  
466 pandas and matplotlib modules for the Python programming language.

467

#### 468 **Cell growth assay**

469 We set up three or four 1,000 mL roller bottles with 90 mL of 7H9 ADC and 10 mL  
470 borosilicate beads. Each bottle was inoculated with a volume of starter cultures so that the initial  
471 bacterial density was at an  $OD_{600}$  of  $5 \times 10^{-7}$ . The inoculated bottles were then placed in a roller  
472 incubator set to 37°C, and incubated for 12 to 18 days with continuous rolling.  $OD_{600}$   
473 measurements were taken once or twice every 24 hours. Two independent experiments in either  
474 triplicates or quadruplates were performed per strain.

475 We defined the exponential phase as the bacterial growth phase where we observed a  
476  $\log_2$ -linear relationship between  $OD_{600}$  and time; specifically, we used a Pearson's  $R^2$  value  $\geq$   
477 0.98 as the threshold. The growth rate of a particular strain was then defined as the slope of the  
478 linear regression model. The relative fitness of a given spontaneous OFX-R mutant was defined  
479 by taking the growth rate of the OFX-resistant mutant strain and dividing it by the growth rate of  
480 its respective drug-susceptible ancestor. Linear regression models for the cell growth assays data  
481 were performed using the numpy, scipy, pandas and matplotlib modules for the Python  
482 programming language, as well as the R statistical software (70).

483

#### 484 **Surveying the fluoroquinolone-resistance profile from publicly available *M. tuberculosis*** 485 **genomes**

486 We screened public databases to download global representatives of *Mtb* genomes, as  
487 described by Menardo *et al.* (74). We selected genomes that were classified as MDR-TB based

488 on the presence of both isoniazid (INH)- and rifampicin (RIF)-resistance mutations. This  
489 provided a dataset of 3,452 genomes with confirmed MDR-TB; their accession numbers are  
490 reported in Table S8 (See SI Appendix). These MDR-TB genomes were then screened for the  
491 presence of FQ-resistance mutations, and we identified 854 genomes that were classified as FQ-  
492 R.

493 The INH-, RIF-, and FQ-resistance mutations used for screening are the same mutations  
494 used by Payne, Menardo *et al.* (75), and are listed in Table S12 (See SI Appendix). A drug-  
495 resistance mutation was defined as “fixed” in the population when it reached a frequency of  
496  $\geq 90\%$ . Meanwhile, a drug-resistance mutation was considered “variable” in the population when  
497 its frequency was between 10% to 90%; thus, multiple drug-resistance mutations may be present  
498 in the genomic data from a single *Mtb* clinical isolate.

499

## 500 **Acknowledgements**

501 The authors would like to thank Sebastian Bonhoeffer, Daniel Angst, and Diarmaid Hughes for  
502 providing critical comments on the manuscript. Calculations were performed at sciCORE  
503 (<http://scicore.unibas.ch/>) scientific computing core facility at University of Basel. Library  
504 preparation and sequencing was carried out in the Genomics Facility Basel. This work was  
505 supported by the Swiss National Science Foundation (grants 310030\_166687, IZRJZ3\_164171,  
506 IZLSZ3\_170834 and CRSII5\_177163), the European Research Council (309540-EVODRTB)  
507 and SystemsX.ch.

508

## 509 **References**

510 1. MacGowan AP (2008) Clinical implications of antimicrobial resistance for therapy. *J*  
511 *Antimicrob Chemother* 62(Suppl\_2):ii105-ii114.

512 2. Winston CA, Mitruka K (2002) Treatment duration for patients with drug-resistant  
513 tuberculosis, United States. *Emerg Infect Dis* 18(7):1201–1202.

514 3. Dalton T, et al. (2012) Prevalence of and risk factors for resistance to second-line drugs in  
515 people with multidrug-resistant tuberculosis in eight countries: a prospective cohort study. *The*  
516 *Lancet* 380(9851):1406–1417.

517 4. Merker M, et al. (2015) Evolutionary history and global spread of the *Mycobacterium*  
518 *tuberculosis* Beijing lineage. *Nat Genet* 47(3):242–249.

519 5. Alvarez-Uria G, Gandra S, Laxminarayan R (2016) Poverty and prevalence of  
520 antimicrobial resistance in invasive isolates. *Int J Infect Dis* 52:59–61.

521 6. Eldholm V, et al. (2016) Armed conflict and population displacement as drivers of the  
522 evolution and dispersal of *Mycobacterium tuberculosis*. *Proc Natl Acad Sci* 113(48):13881–  
523 13886.

524 7. Shah NS, et al. (2017) Transmission of Extensively Drug-Resistant Tuberculosis in South  
525 Africa. *N Engl J Med* 376(3):243–253.

526 8. zur Wiesch PA, Kouyos R, Engelstädtter J, Regoes RR, Bonhoeffer S (2011) Population  
527 biological principles of drug-resistance evolution in infectious diseases. *Lancet Infect Dis*  
528 11(3):236–247.

529 9. Hughes D, Andersson DI (2017) Evolutionary Trajectories to Antibiotic Resistance. *Annu*  
530 *Rev Microbiol* 71(1):579–596.

531 10. Zhou J, et al. (2000) Selection of Antibiotic-Resistant Bacterial Mutants: Allelic Diversity  
532 among Fluoroquinolone-Resistant Mutations. *J Infect Dis* 182(2):517–525.

533 11. Ford CB, et al. (2013) *Mycobacterium tuberculosis* mutation rate estimates from different  
534 lineages predict substantial differences in the emergence of drug-resistant tuberculosis. *Nat Genet*  
535 45(7):784–790.

536 12. Lindsey HA, Gallie J, Taylor S, Kerr B (2013) Evolutionary rescue from extinction is  
537 contingent on a lower rate of environmental change. *Nature* 494(7438):463–467.

538 13. McGrath M, Gey van Pittius NC, van Helden PD, Warren RM, Warner DF (2014)  
539 Mutation rate and the emergence of drug resistance in *Mycobacterium tuberculosis*. *J Antimicrob*  
540 *Chemother* 69(2):292–302.

541 14. Huseby DL, et al. (2017) Mutation Supply and Relative Fitness Shape the Genotypes of  
542 Ciprofloxacin-Resistant *Escherichia coli*. *Mol Biol Evol* 34(5):1029–1039.

543 15. Fenner L, et al. (2012) Effect of Mutation and Genetic Background on Drug Resistance in  
544 *Mycobacterium tuberculosis*. *Antimicrob Agents Chemother* 56(6):3047–3053.

545 16. Vogwill T, Kojadinovic M, Furió V, MacLean RC (2014) Testing the Role of Genetic  
546 Background in Parallel Evolution Using the Comparative Experimental Evolution of Antibiotic  
547 Resistance. *Mol Biol Evol* 31(12):3314–3323.

548 17. Gagneux S (2018) Ecology and evolution of *Mycobacterium tuberculosis*. *Nat Rev*  
549 *Microbiol* 16(4):202–213.

550 18. Ängeby KA, et al. (2010) Wild-type MIC distributions of four fluoroquinolones active  
551 against *Mycobacterium tuberculosis* in relation to current critical concentrations and available  
552 pharmacokinetic and pharmacodynamic data. *J Antimicrob Chemother* 65(5):946–952.

553 19. Coeck N, et al. (2016) Correlation of different phenotypic drug susceptibility testing  
554 methods for four fluoroquinolones in *Mycobacterium tuberculosis*. *J Antimicrob Chemother*  
555 71(5):1233–1240.

556 20. Colangeli R, et al. (2018) Bacterial Factors That Predict Relapse after Tuberculosis  
557 Therapy. *N Engl J Med* 379(9):823–833.

558 21. Borrell S, Gagneux S (2009) Infectiousness, reproductive fitness and evolution of drug-  
559 resistant *Mycobacterium tuberculosis*. *Int J Tuberc Lung Dis Off J Int Union Tuberc Lung Dis*  
560 13(12):1456–1466.

561 22. Wollenberg KR, et al. (2017) Whole-Genome Sequencing of *Mycobacterium tuberculosis*  
562 Provides Insight into the Evolution and Genetic Composition of Drug-Resistant Tuberculosis in  
563 Belarus. *J Clin Microbiol* 55(2):457–469.

564 23. Oppong YEA, et al. (2019) Genome-wide analysis of *Mycobacterium tuberculosis*  
565 polymorphisms reveals lineage-specific associations with drug resistance. *BMC Genomics*  
566 20(1):252.

567 24. Gagneux S, et al. (2006) The Competitive Cost of Antibiotic Resistance in  
568 *Mycobacterium tuberculosis*. *Science* 312(5782):1944–1946.

569 25. Decuypere S, et al. (2012) Molecular Mechanisms of Drug Resistance in Natural  
570 Leishmania Populations Vary with Genetic Background. *PLoS Negl Trop Dis* 6(2):e1514.

571 26. Angst DC, Hall AR (2013) The cost of antibiotic resistance depends on evolutionary  
572 history in *Escherichia coli*. *BMC Evol Biol* 13(1):163.

573 27. Vogwill T., Kojadinovic M., MacLean R. C. (2016) Epistasis between antibiotic  
574 resistance mutations and genetic background shape the fitness effect of resistance across species  
575 of *Pseudomonas*. *Proc R Soc B Biol Sci* 283(1830):20160151.

576 28. Trauner A, et al. (2018) Resource misallocation as a mediator of fitness costs in antibiotic  
577 resistance. *bioRxiv*:456434.

578 29. World Health Organization (2017) *Global tuberculosis report 2018* (Geneva,  
579 Switzerland) Available at: [https://www.who.int/tb/publications/global\\_report/en/](https://www.who.int/tb/publications/global_report/en/).

580 30. Comas I, et al. (2010) Human T cell epitopes of *Mycobacterium tuberculosis* are  
581 evolutionarily hyperconserved. *Nat Genet* 42(6):498–503.

582 31. Zaczek A, Brzostek A, Augustynowicz-Kopec E, Zwolska Z, Dziadek J (2009) Genetic  
583 evaluation of relationship between mutations in *rpoB* and resistance of *Mycobacterium*  
584 *tuberculosis* to rifampin. *BMC Microbiol* 9(1):10.

585 32. Imperial MZ, et al. (2018) A patient-level pooled analysis of treatment-shortening  
586 regimens for drug-susceptible pulmonary tuberculosis. *Nat Med* 24(11):1708–1715.

587 33. Vjecha MJ, Tiberi S, Zumla A (2018) Accelerating the development of therapeutic  
588 strategies for drug-resistant tuberculosis. *Nat Rev Drug Discov* 17(5):377.

589 34. Gillespie SH, et al. (2014) Four-Month Moxifloxacin-Based Regimens for Drug-Sensitive  
590 Tuberculosis. *N Engl J Med* 371(17):1577–1587.

591 35. Jindani A, et al. (2014) High-Dose Rifapentine with Moxifloxacin for Pulmonary  
592 Tuberculosis. *N Engl J Med* 371(17):1599–1608.

593 36. Merle CS, et al. (2014) A Four-Month Gatifloxacin-Containing Regimen for Treating  
594 Tuberculosis. *N Engl J Med* 371(17):1588–1598.

595 37. Takiff H, Guerrero E (2011) Current Prospects for the Fluoroquinolones as First-Line  
596 Tuberculosis Therapy. *Antimicrob Agents Chemother* 55(12):5421–5429.

597 38. Takiff HE, et al. (1994) Cloning and nucleotide sequence of *Mycobacterium tuberculosis*  
598 *gyrA* and *gyrB* genes and detection of quinolone resistance mutations. *Antimicrob Agents*  
599 *Chemother* 38(4):773–780.

600 39. Maruri F, et al. (2012) A systematic review of gyrase mutations associated with  
601 fluoroquinolone-resistant *Mycobacterium tuberculosis* and a proposed gyrase numbering system.  
602 *J Antimicrob Chemother* 67(4):819–831.

603 40. Rigouts L, et al. (2016) Specific *gyrA* gene mutations predict poor treatment outcome in  
604 MDR-TB. *J Antimicrob Chemother* 71(2):314–323.

605 41. Piton J, et al. (2010) Structural Insights into the Quinolone Resistance Mechanism of  
606 *Mycobacterium tuberculosis* DNA Gyrase. *PLOS ONE* 5(8):e12245.

607 42. Aldred KJ, Blower TR, Kerns RJ, Berger JM, Osheroff N (2016) Fluoroquinolone  
608 interactions with *Mycobacterium tuberculosis* gyrase: Enhancing drug activity against wild-type  
609 and resistant gyrase. *Proc Natl Acad Sci* 113(7):E839–E846.

610 43. Blower TR, Williamson BH, Kerns RJ, Berger JM (2016) Crystal structure and stability  
611 of gyrase–fluoroquinolone cleaved complexes from *Mycobacterium tuberculosis*. *Proc Natl Acad  
612 Sci* 113(7):1706–1713.

613 44. Boritsch EC, et al. (2016) Key experimental evidence of chromosomal DNA transfer  
614 among selected tuberculosis-causing mycobacteria. *Proc Natl Acad Sci* 113(35):9876–9881.

615 45. Gygli SM, Borrell S, Trauner A, Gagneux S (2017) Antimicrobial resistance in  
616 *Mycobacterium tuberculosis*: mechanistic and evolutionary perspectives. *FEMS Microbiol Rev*  
617 41(3):354–373.

618 46. Mustaev A, et al. (2014) Fluoroquinolone-Gyrase-DNA Complexes TWO MODES OF  
619 DRUG BINDING. *J Biol Chem* 289(18):12300–12312.

620 47. Malik M, et al. (2016) Suppression of gyrase-mediated resistance by C7 aryl  
621 fluoroquinolones. *Nucleic Acids Res* 44(7):3304–3316.

622 48. Luria SE, Delbrück M (1943) Mutations of Bacteria from Virus Sensitivity to Virus  
623 Resistance. *Genetics* 28(6):491–511.

624 49. Borrell S, et al. (2019) Reference set of *Mycobacterium tuberculosis* clinical strains: A  
625 tool for research and product development. *PLOS ONE* 14(3):e0214088.

626 50. Rock JM, et al. (2015) DNA replication fidelity in *Mycobacterium tuberculosis* is  
627 mediated by an ancestral prokaryotic proofreader. *Nat Genet* 47(6):677–681.

628 51. Baños-Mateos S, et al. (2017) High-fidelity DNA replication in *Mycobacterium*  
629 tuberculosis relies on a trinuclear zinc center. *Nat Commun* 8(1):855.

630 52. Wengren J, Hoffner SE (2003) Drug-Susceptible *Mycobacterium tuberculosis* Beijing  
631 Genotype Does Not Develop Mutation-Conferred Resistance to Rifampin at an Elevated Rate. *J*  
632 *Clin Microbiol* 41(4):1520–1524.

633 53. Malik M, Hoatam G, Chavda K, Kerns RJ, Drlica K (2010) Novel Approach for  
634 Comparing the Abilities of Quinolones To Restrict the Emergence of Resistant Mutants during  
635 Quinolone Exposure. *Antimicrob Agents Chemother* 54(1):149–156.

636 54. Borrell S, et al. (2013) Epistasis between antibiotic resistance mutations drives the  
637 evolution of extensively drug-resistant tuberculosis. *Evol Med Public Health* 2013(1):65–74.

638 55. Farhat MR, et al. (2017) Fluoroquinolone Resistance Mutation Detection Is Equivalent to  
639 Culture-Based Drug Sensitivity Testing for Predicting Multidrug-Resistant Tuberculosis  
640 Treatment Outcome: A Retrospective Cohort Study. *Clin Infect Dis* 65(8):1364–1370.

641 56. Stucki D, et al. (2016) *Mycobacterium tuberculosis* lineage 4 comprises globally  
642 distributed and geographically restricted sublineages. *Nat Genet* 48(12):1535–1543.

643 57. Brynildsrud OB, et al. (2018) Global expansion of *Mycobacterium tuberculosis* lineage 4  
644 shaped by colonial migration and local adaptation. *Sci Adv* 4(10):eaat5869.

645 58. Pienaar E, et al. (2017) Comparing efficacies of moxifloxacin, levofloxacin and  
646 gatifloxacin in tuberculosis granulomas using a multi-scale systems pharmacology approach.  
647 *PLOS Comput Biol* 13(8):e1005650.

648 59. Sarathy JP, et al. (2018) Extreme Drug Tolerance of *Mycobacterium tuberculosis* in  
649 Caseum. *Antimicrob Agents Chemother* 62(2):e02266-17.

650 60. Handel A, Margolis E, Levin BR (2009) Exploring the role of the immune response in  
651 preventing antibiotic resistance. *J Theor Biol* 256(4):655–662.

652 61. Cirz RT, et al. (2005) Inhibition of Mutation and Combating the Evolution of Antibiotic  
653 Resistance. *PLOS Biol* 3(6):e176.

654 62. Frenoy A, Bonhoeffer S (2018) Death and population dynamics affect mutation rate  
655 estimates and evolvability under stress in bacteria. *PLOS Biol* 16(5):e2005056.

656 63. Comas I, et al. (2012) Whole-genome sequencing of rifampicin-resistant *Mycobacterium*  
657 *tuberculosis* strains identifies compensatory mutations in RNA polymerase genes. *Nat Genet*  
658 44(1):106–110.

659 64. Barrick JE, Lenski RE (2013) Genome dynamics during experimental evolution. *Nat Rev*  
660 *Genet* 14(12):827–839.

661 65. Hershberg R, et al. (2008) High Functional Diversity in *Mycobacterium tuberculosis*  
662 Driven by Genetic Drift and Human Demography. *PLOS Biol* 6(12):e311.

663 66. de Vos M, et al. (2013) Putative Compensatory Mutations in the rpoC Gene of Rifampin-  
664 Resistant *Mycobacterium tuberculosis* Are Associated with Ongoing Transmission. *Antimicrob*  
665 *Agents Chemother* 57(2):827–832.

666 67. Casali N, et al. (2014) Evolution and transmission of drug-resistant tuberculosis in a  
667 Russian population. *Nat Genet* 46(3):279–286.

668 68. Gagneux S, et al. (2006) Variable host-pathogen compatibility in *Mycobacterium*  
669 *tuberculosis*. *Proc Natl Acad Sci* 103(8):2869–2873.

670 69. Rosche WA, Foster PL (2000) Determining Mutation Rates in Bacterial Populations.  
671 *Methods* 20(1):4–17.

672 70. R Core Team (2018) *R: A language and environment for statistical computing*. (R  
673 Foundation for Statistical Computing, Vienna, Austria) Available at: <https://www.r-project.org/>.

674 71. Feuerriegel S, et al. (2009) Sequence Analyses of Just Four Genes To Detect Extensively  
675 Drug-Resistant *Mycobacterium tuberculosis* Strains in Multidrug-Resistant Tuberculosis Patients  
676 Undergoing Treatment. *Antimicrob Agents Chemother* 53(8):3353–3356.

677 72. Cole ST, et al. (1998) Deciphering the biology of *Mycobacterium tuberculosis* from the  
678 complete genome sequence. *Nature* 393(6685):537–544.

679 73. Franzblau SG, et al. (1998) Rapid, Low-Technology MIC Determination with Clinical  
680 *Mycobacterium tuberculosis* Isolates by Using the Microplate Alamar Blue Assay. *J Clin*  
681 *Microbiol* 36(2):362–366.

682 74. Menardo F, et al. (2018) Treemmer: a tool to reduce large phylogenetic datasets with  
683 minimal loss of diversity. *BMC Bioinformatics* 19(1):164.

684 75. Payne JL, et al. (2019) Transition bias influences the evolution of antibiotic resistance in  
685 *Mycobacterium tuberculosis*. *PLOS Biol* 17(5):e3000265.

686

687 **Figure Legends**

688 **Fig. 1**

689 Variation in the frequency of ofloxacin-resistance between genetically distinct, wild-type *M.*  
690 *tuberculosis* strains. **A.** Frequency of ofloxacin-resistance at 4 µg/mL ofloxacin (OFX), as

691 measured by fluctuation analysis. Top panel: Coloured points represent the frequency of resistant  
692 mutants per cell per parallel culture, with darker points representing multiple cultures with the  
693 same frequency. Colours denote the lineage that the *M. tuberculosis* strain belongs to (L1 = pink;  
694 L2 = blue; L4 = red). Grey points represent the estimated number of mutations per cell per strain  
695 as calculated by MSS-MLE, while black bars denote the respective 95% confidence intervals.  
696 Bottom panel: the percentage of parallel cultures lacking OFX-resistant mutants. **B.** Frequency of  
697 ofloxacin-resistance at 2 or 8  $\mu$ g/mL OFX.

698

699 **Fig. 2**

700 Frequency of streptomycin-resistance at 100  $\mu$ g/mL streptomycin (STR) for wild-type N0157,  
701 N1283, and N0145 *M. tuberculosis* strains, as measured by fluctuation analysis assay. Top panel:  
702 Coloured points represent the frequency of resistant mutants per cell per parallel culture, with  
703 darker points representing multiple cultures with the same frequency. Colours denote the lineage  
704 that the *M. tuberculosis* strain belongs to (L1 = pink; L2 = blue; L4 = red). Grey points represent  
705 the estimated number of mutations per cell per strain as calculated by MSS-MLE, while black  
706 bars denote the respective 95% confidence intervals. Bottom panel: the percentage of parallel  
707 cultures lacking STR-resistant mutants. Two biological replicates are presented for each *M.*  
708 *tuberculosis* strain, with each replicate identifier suffixed after the strain name.

709

710 **Fig. 3**

711 Variation in the mutational profile for ofloxacin-resistance after fluctuation analyses using nine  
712 genetically-distinct *M. tuberculosis* strains. **A.** Mutations in the quinolone-resistance-determining  
713 region (QRDR) of *gyrA* was analyzed in 680 ofloxacin (OFX)-resistant colonies from the

714 fluctuation analysis performed in Fig. 2A (nm = no identified QRDR *gyrA* mutations). Strains are  
715 ordered left to right based on their frequency of OFX-resistance at 4  $\mu$ g/mL OFX. Numbers of  
716 colonies analyzed per strain are reported directly above each column. **B.** The number of unique  
717 QRDR *gyrA* mutations per *M. tuberculosis* strain for OFX-resistance. Bar colours denote the *M.*  
718 *tuberculosis* lineage the strain belongs to (L1 = pink; L2 = blue; L4 = red).

719

720 **Fig. 4**

721 Ofloxacin (OFX) MIC is modulated by the genetic background of *M. tuberculosis*. **A.** Heat-map  
722 of OFX-susceptibility via Alamar Blue assay for *gyrA* mutant strains of *M. tuberculosis*, as well  
723 as their wild-type ancestor, in three genetic backgrounds (N0157, N0145, or N1283). Light areas  
724 represent growing cultures, while dark areas represent non-growing cultures. Yellow points  
725 represent estimates for OFX MIC ( $\geq 95\%$  reduction in fluorescence). Areas of solid black colours  
726 (at 16+  $\mu$ g/ml OFX for wild-type) and solid yellow colours (at <0.125  $\mu$ g/ml OFX for mutants)  
727 were not measured and coloured in for illustrative purposes. **B.** OFX MIC estimates for each  
728 strain per genetic background, superimposed. Coloured points and lines represent MIC  
729 measurements for highlighted genetic background, with the line colour denoting the lineage that  
730 the strain belongs to (L1 = pink, L2 = blue, L4 = red). Grey points and lines represent the other  
731 two genetic backgrounds.

732

733 **Fig. 5**

734 The *M. tuberculosis* genetic background modulates the fitness effect of fluoroquinolone-  
735 resistance mutations. **A.** Fitness of ofloxacin-resistant *M. tuberculosis* strain with specified *gyrA*  
736 mutation relative to the fitness of their respective wild-type ancestral strain. Ancestral strain per

737 *gyrA* mutant is indicated in the grey bar above each panel. Fitness was measured by cell growth  
738 assay in antibiotic-free conditions. **B.** Association between the relative fitness of specified *gyrA*  
739 mutant and their absolute frequency during the fluctuation analysis performed in Fig. 1A, in three  
740 genetic backgrounds (N0157, N1283, and N0145).

741

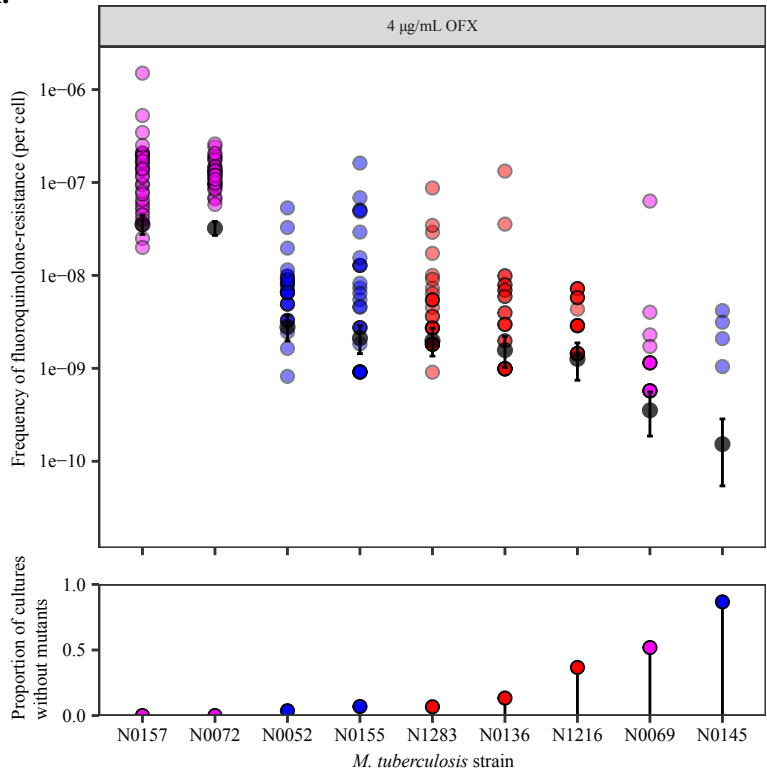
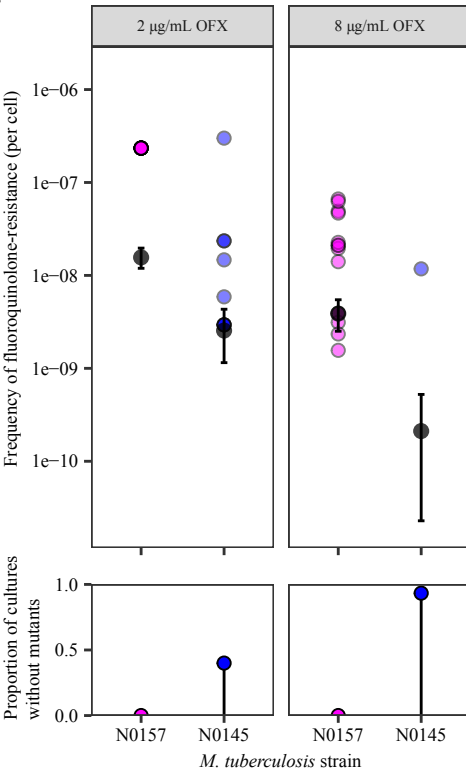
742 **Fig. 6**

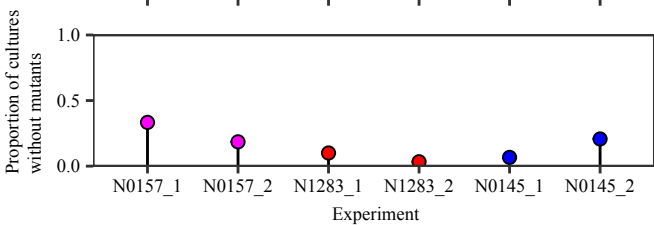
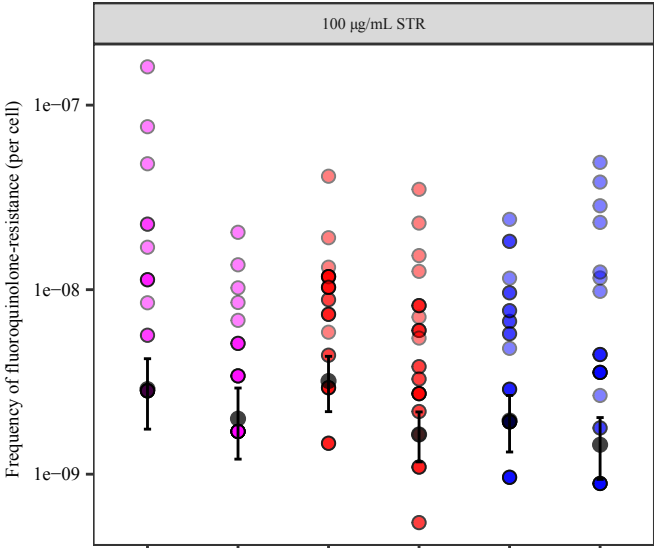
743 Mutational profile for fluoroquinolone-resistance *gyrA* mutations in clinical isolates of *M.*  
744 *tuberculosis*, per lineage. An initial dataset consisting of 3,452 genomes with confirmed MDR-  
745 TB mutations were surveyed. 854 genomes were identified as fluoroquinolone-resistant, with 848  
746 of these genomes containing *gyrA* mutations. Only fixed fluoroquinolone-resistance mutations in  
747 the *gyrA* gene are enumerated here ( $n = 710$ ). No fixed mutations were observed in L5 strains.  
748 Numbers of genomes analyzed per lineage are presented directly below their respective bar  
749 graph.

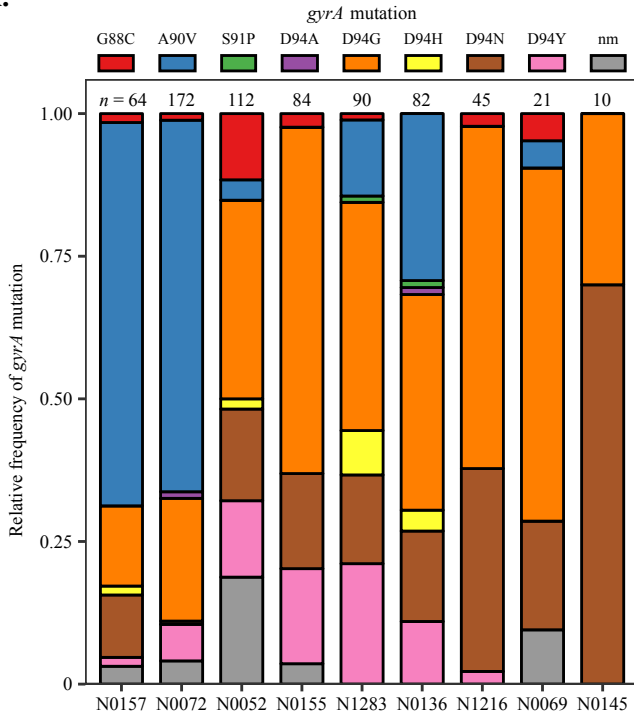
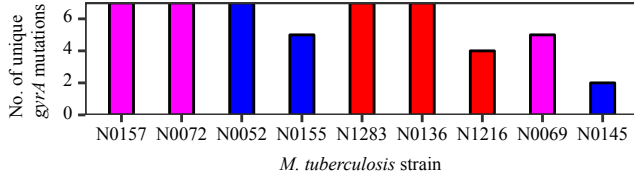
750

751 **Fig. 7**

752 Association between the clinical frequencies of fluoroquinolone-resistance *gyrA* mutations with  
753 their respective *in vitro* frequencies amongst *M. tuberculosis* strains belonging to either the L2 or  
754 L4 lineages. Clinical frequencies are identical as reported in Fig. 6, while the *in vitro* frequencies  
755 are the same as in Fig. 3A, grouped by lineage.

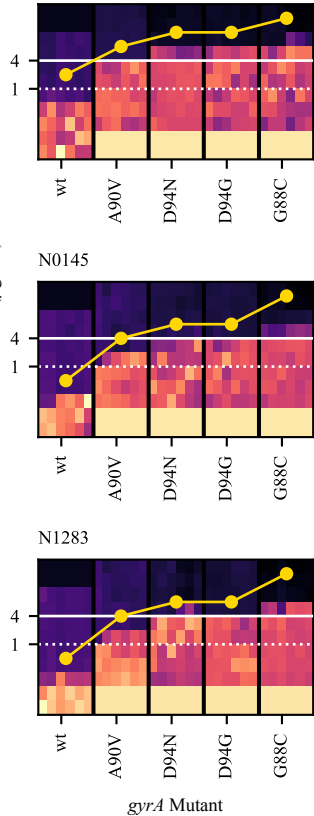
**A.****B.**



**A.****B.**

**A.**

N0157

Ofloxacin concentration ( $\mu\text{g/mL}$ )**B.**

N0157

10<sup>1</sup>10<sup>0</sup>10<sup>-1</sup>10<sup>-2</sup>10<sup>-3</sup>10<sup>-4</sup>10<sup>-5</sup>10<sup>-6</sup>10<sup>-7</sup>10<sup>-8</sup>10<sup>-9</sup>10<sup>-10</sup>10<sup>-11</sup>10<sup>-12</sup>10<sup>-13</sup>10<sup>-14</sup>10<sup>-15</sup>10<sup>-16</sup>10<sup>-17</sup>10<sup>-18</sup>10<sup>-19</sup>10<sup>-20</sup>10<sup>-21</sup>

N0145

10<sup>1</sup>10<sup>0</sup>10<sup>-1</sup>10<sup>-2</sup>10<sup>-3</sup>10<sup>-4</sup>10<sup>-5</sup>10<sup>-6</sup>10<sup>-7</sup>10<sup>-8</sup>10<sup>-9</sup>10<sup>-10</sup>10<sup>-11</sup>10<sup>-12</sup>10<sup>-13</sup>10<sup>-14</sup>10<sup>-15</sup>

N0145

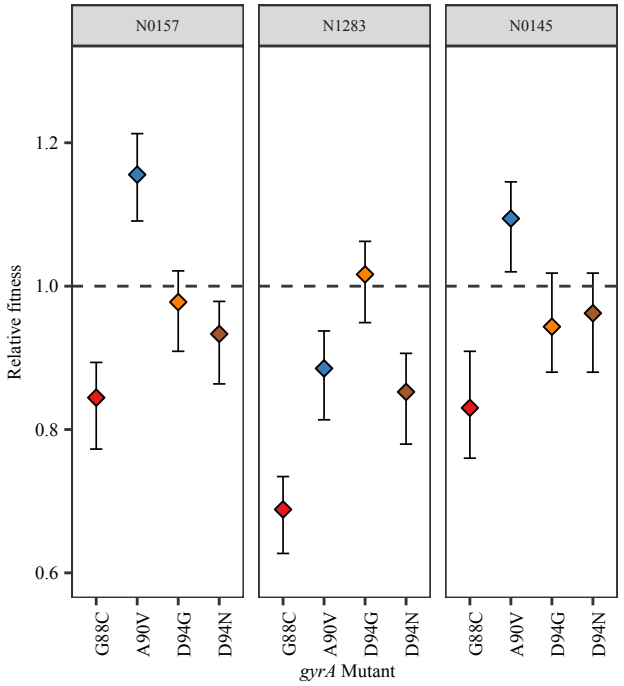
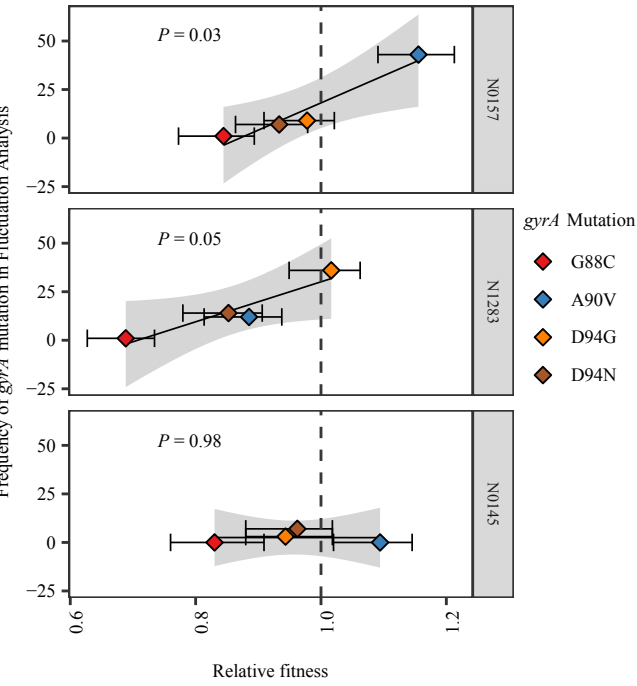
10<sup>1</sup>10<sup>0</sup>10<sup>-1</sup>10<sup>-2</sup>10<sup>-3</sup>10<sup>-4</sup>10<sup>-5</sup>10<sup>-6</sup>10<sup>-7</sup>10<sup>-8</sup>10<sup>-9</sup>10<sup>-10</sup>10<sup>-11</sup>10<sup>-12</sup>10<sup>-13</sup>10<sup>-14</sup>10<sup>-15</sup>

N1283

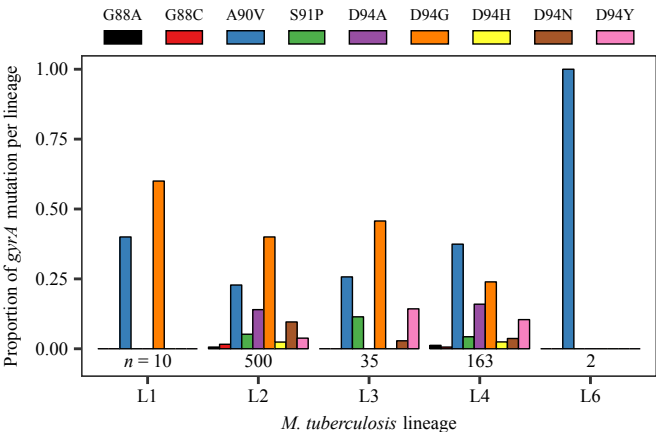
10<sup>1</sup>10<sup>0</sup>10<sup>-1</sup>10<sup>-2</sup>10<sup>-3</sup>10<sup>-4</sup>10<sup>-5</sup>10<sup>-6</sup>10<sup>-7</sup>10<sup>-8</sup>10<sup>-9</sup>10<sup>-10</sup>10<sup>-11</sup>10<sup>-12</sup>10<sup>-13</sup>10<sup>-14</sup>10<sup>-15</sup>

N1283

10<sup>1</sup>10<sup>0</sup>10<sup>-1</sup>10<sup>-2</sup>10<sup>-3</sup>10<sup>-4</sup>10<sup>-5</sup>10<sup>-6</sup>10<sup>-7</sup>10<sup>-8</sup>10<sup>-9</sup>10<sup>-10</sup>10<sup>-11</sup>10<sup>-12</sup>10<sup>-13</sup>10<sup>-14</sup>10<sup>-15</sup>*gyra* Mutant*gyra* Mutant

**A.****B.**

### *gyrA* mutation



*gyrA* Mutation

G88A G88C A90V S91P D94A D94G D94H D94N D94Y

Frequency of *gyrA* mutation from clinical genomic data